Detection of Dose Concentration in Droplets Generated by Pulmonary Drug Delivery Devices

Cary Presser[*]
Chemical Science and Technology Laboratory
National Institute of Standards and Technology
Gaithersburg, MD 20899-8360 USA

Abstract

Using aerosol delivery devices to administer new therapeutic drugs through the pulmonary system is emerging as an efficacious way to engage several diseases. Little quantitative information on spatially or temporally resolved concentration of the drug throughout the aerosol (i.e., presence of the active agent within any particular droplet) is available; concentration along with droplet size is critical for proper dosage and transport efficiency to the site of action. The importance of such measurements is even more acute in suspensions (or colloids) where drug can float, settle, or agglomerate, adhere to surfaces, and contribute to inconsistent medication dose delivery and particle size distribution. In this study, a measurement approach was developed to obtain droplet dose concentration of pharmaceutical-laden, multiphase aerosols. Since many biological molecules either are naturally fluorescent or can be chemically modified with fluorophores, one can relate fluorescence intensity to concentration (or mass) of these inclusions within the droplet volume. The approach used distinguishes between aerosol droplets that may or may not contain fluorescing agent (i.e., to identify droplet-to-droplet variations in agent concentration). The results demonstrate how one can identify fluorescing droplets using this approach.

[*]Corresponding author

Introduction

Determining concentration of suspended material in droplets of an aerosolized heterogeneous mixture is a generic problem that exists in several different industries such as in law enforcement (e.g., in the delivery of pepper sprays), homeland security and environmental health (e.g., in the dispersion of chemical and pathogenic aerosols), climate change (e.g., in the formation atmospheric aerosols and clouds), and materials processes (e.g., in the coating of surfaces). This issue is gaining recognition in the health care industry with respect to delivery of new pharmaceutical drugs with formulations that are emulsions with immiscible components that may settle out of solution.

The US drug delivery market was estimated to be over $74.4 billion in 2006 and is expected to grow and reach $91 billion by 2009 and $153.5 billion by 2011 [1]. About 15 % of the current market (~$13 billion) includes pulmonary drug delivery systems, which is also expected to continue to grow. Although no roadmap for the biopharmaceutical industry currently exists, work is progressing that parallels the semiconductor industry and recognizes the need for 'better product characterization and improved process understanding' [2]. More than 300 biotechnology, generic, and specialty pharmaceutical drugs are currently in development to address an ever-increasing variety of respiratory and nonrespiratory diseases via pulmonary delivery.

The lung offers an enormous surface area (75 m^2/70 kg person [3]) with straightforward drug penetration and transport across the alveoli (epithelial cells of ~0.1 mm) to the bloodstream for quick delivery to major organs. Pulmonary drug delivery avoids first–pass metabolism by the liver and thus leaves drugs in tact. Also, both small and large molecular weight molecules can be delivered and dosages can be small to minimize side effects. Many of the new drug formulations slated for pulmonary delivery are multiphase micro-emulsions with limited solubility or dispersed particles that may settle out of solution after a period of time, and thus require novel and complex aerosol delivery techniques [4].

Diseases addressed include respiratory infections, asthma, COPD (chronic obstructive pulmonary disease), cystic fibrosis, emphysema, and ARDS (acute respiratory distress syndrome). In more recent years inhalation therapy has been used to address diabetes (e.g., Exubera [5, 6]; inhaled insulin sales were expected to reach $2 billion in 2007 [7], however, poor sales has recently removed the product from the market while companies continue development [5]), and for treating the immune system, such as for allergies (with the steroid Flonaze), viral infections (e.g., Ribavirin [4]), and vaccines (e.g., FluMist for the flu). Research into new applications of inhalation delivery methods includes gene therapy via tissue targeting and organ targeting [8], multiple sclerosis, and treating hepatitis B and C with interferons. Other diseases may be addressed by inhalation of peptides and proteins, such as with hormones for fertility, and osteoporosis (with the peptide PTH) [9].

Pulmonary drug delivery is controlled largely by aerosol characteristics; in particular, droplet size and velocity for respiratory applications, for which droplets of size smaller than 1 μm are likely to be exhaled, and droplets greater than 10 μm tend to coat the trachea wall. Recent studies have shown that only 20 % to 50 % of injected aerosol often reaches the lung due to coating of surfaces within the nebulizer and exhalation. In a recent study, a dry powder type inhaler that used a breath controlled drug delivery system was found to increase significantly delivery of the therapeutic drug [10]. An improvement in delivered dosage was achieved by controlling humidity in a surrogate model lung [3]. For the size range of 1 μm to 10 μm, droplets have the highest probability of reaching the deep lung during inhalation.

Improving dosing consistency remains a major issue for drug delivery companies [4]. The general classes of delivery devices

include metered dose inhalers, dry powder inhalers, and nebulizers (aerosolize water-soluble materials with a wide droplet size distribution). An optimized drug delivery strategy can improve performance of therapeutic molecules by increasing efficacy and reducing side effects, and reduce costs for expensive drugs of limited supply [11]. State-of-the-art characterization of inhalers and nebulizers includes laser diffraction (e.g., Ref. [12]), phase Doppler interferometry (e.g., Ref. [13]), and intrusive collection of particles for chemical and morphological analysis [14].

Little quantitative information on spatially or temporally resolved concentration of the therapeutic drug throughout the aerosol (i.e., presence of the active agent within any particular droplet) is available in the literature [15], which along with droplet size is critical for proper dosage and transport efficiency to the site of action. The importance of such measurements is even more acute in suspension where drug can float, settle, or agglomerate, adhere to surfaces, and contribute to inconsistent medication dose delivery [16, 17]. In this study, our objective was to develop a measurement approach to obtain droplet dose concentration of pharmaceutical-laden, multiphase aerosols. Since many biological molecules either are naturally fluorescent or can be chemically modified with fluorophores, one can relate fluorescence intensity to concentration (or mass) of these inclusions within the droplet volume. In addition, one can conceive of using fluorescent molecules as surrogates for new pharmaceutical agents to characterize the homogeneity of suspended material within droplets.

Experimental Arrangement

The measurement approach uses laser-induced fluorescence microscopy and a concomitant set of optics to provide spatially and temporally resolved detection of the drug within inhaler aerosol droplets. Fluorescence is considered because many pharmaceutical components such as biological molecules that are naturally fluorescent or can be chemically modified with biomarkers (e.g., fluorophores, and quantum dots), are being used with increasing frequency [18, 19]. The approach builds upon the concept of the optical patternator [20, 21] in which both fluorescence and Mie scattered light are detected from soluble fluorescent-doped liquid droplets of a spray, using a laser sheet and digital camera. The objective in optical patternation is to detect all droplets so as to determine the spray total mass flux. Our interests lie in determining the droplet concentration distribution with droplet size by detecting individual fluorescing droplets. Thus, our approach is applicable to both soluble droplet mixtures, as well as heterogeneous multiphase droplets.

Our methodology monitors the presence of pharmaceuticals within multiphase droplets that are generated by aerosol inhalers. Fluorescence microscopy is employed to distinguish between droplets of an aerosolized solution (i.e., composed of propellant, carrier liquid, and active agent) with and without active agent. A schematic and photograph of the current experimental arrangement is presented in Fig. 1. Millimeter-sized pendent droplets and different precision pinholes (ranging from 100 μm down to 2 μm) were used to align the laser beam and optics, and estimate the resolution of the optical arrangement. In our simplified arrangement, a commercially available vibrating orifice aerosol generator was used to provide a single stream of droplets. A Nd:YAG pulsed laser was used as the illuminating source (operating at a wavelength of 532 nm, laser fluence of 300 mJ, repetition rate of 10 Hz, pulse duration of 5 ns, and Q-switch delay of 184 μs), in which the beam excites fluorescence of the agent within a droplet.

Light is scattered when a droplet from the array generator, or a cross section of droplets within an inhaler aerosol, traverses the laser beam. The scattered light is collected through a beam splitter cube, which forms two images of each droplet 10 mm apart. A laser long-pass filter ($\lambda > 550$ nm) is placed in front of one image; the filter absorbs the incident

elastic light at the laser wavelength and transmits inelastic fluorescent light. Thus, if a droplet fluoresces then two images will be recorded. If the droplet does not fluoresce, only the unfiltered image of elastically scattered light will be collected. The elastically scattered image acts as a marker for all droplets in the optical field-of-view, while the fluorescence image serves to distinguish between fluorescing (i.e., droplets with active agent) and nonfluorescing droplets. The two images are brought spatially close to one another (to within the field-of-view of a long-distance microscope) by adjusting two right angle prisms, which are positioned as indicated in Fig. 1. This arrangement results in unequal image path lengths, however, imaging from the other prism shown in Fig. 1 (providing equal image path lengths) is more difficult to align within the microscope at the present time. In another arrangement, a beam splitter flat plate is used but with less control of the image splitting and separation distance.

The two images are magnified within a long-distance microscope, which has a resolution of 1.75 μm and field-of-view of 4 mm at the shortest working distance of 102 mm. A 200 mm zoom lens is used to enlarge the image into a 35 mm digital camera or CMOS high-speed movie camera. The CMOS camera has a pixel resolution of 1280 x 1024 and pixel size of 12 μm x 12 μm, and records the detected droplets of the array (or aerosol) on a personal computer that runs image recording and processing software. With this optical arrangement, we are able to image a 2 μm diameter pinhole. The software also controls the synchronous operation of the laser pulse and camera exposure (at the pulse signal leading edge, camera latency of 20 ns, and variable integration time of 100 ms to 1 s), by triggering externally a digital delay/pulse generator, which in turn is used to trigger the laser.

The vibrating orifice aerosol generator was operated at 1 kHz with a 100 μm diameter pinhole using water to generate a linear array of large droplets with an estimated diameter of 375 μm. Note that the laser (operating at 10 Hz) was not synchronized with the generation of the droplet array and thus droplets were illuminated arbitrarily. The relatively large diameter pinhole was used for convenience only. Fluorescence signals were induced within the droplets by laser excitation of a dilute aqueous solution of 10^{-6} M rhodamine B in water. Since the droplets were smaller than the laser beam diameter, which was set at 5 mm with a spatial filter, it was unnecessary to make the laser beam planar because of the smaller microscope viewing region.

To detect the scattered light from each droplet two approaches were available, namely, backscatter illumination of the laser beam directly in the microscope (i.e., laser shadowgraphy) and 90° side-angle scattering. Backscatter illumination results in focusing the laser light to a point so one will view a black circle (representing the perimeter of the droplet) with a light spot in the middle [9]. Side-angle scattering results in a black circle with two luminous spots located 180º apart from one another (i.e., glare points [22]). Either approach was successful in detecting the droplets. Also, note that although liquid droplets are considered here, the approach is also expected to be applicable to dry powder fluorescing particles. In this case, light reflection from the particle would be considered.

Results and Discussion

Results are presented for both the backscatter illumination and side-angle scattering. Figure 2 presents a typical unsplit focused image of droplets traversing the field-of-view, as obtained using backscatter illumination, the array generator and CMOS movie camera. The observed light-focusing effect through the droplets is also illustrated in the figure. The image shows the droplet size and presence of droplet asphericity (not observed with side-angle scattering), as well as droplet coalescence and uneven spacing between droplets.

When the image is split into two, the focal plane of the two images is different for each image due to the difference in optical path length through the beam splitter cube and prisms. This issue is eliminated using a beam splitter flat plate; however, illumination clarity of the back surface reflection is degraded, as well as alignment control of both images within the limited field-of-view. The image focusing effect with the beam splitter cube and prisms is illustrated in Fig. 3, which presents a pendent millimeter-sized water droplet with backscattering from an incandescent lamp, and reduced zoom-lens magnification. Figure 3a emphasizes the focused filtered-path image (without the filter) and Fig. 3c the unfiltered-path image, while Fig. 3b illustrates equal focusing of both images with reduced clarity. Although the recorded images are slightly out of focus with the current arrangement, both images are observable and can serve to detect fluorescing droplets.

The double image of droplets observed in the field-of-view is presented in Fig. 4. Note that the droplet images are highlighted by a white oval for clarity. The darkened region in the middle of Fig. 4a results from the larger spacing between images after adjustment of the prisms. The vertical displacement between image pairs is also due to the prism adjustment. The field-of-view of the two images is aligned next to one another in Figs. 4b and 4c. The images show that multiple droplets can be detected during the flash of the laser, as well as the variation in droplet size and sphericity, and spacing between droplets.

An example of results obtained with the 90° side-angle scattering is presented in Fig. 5. Note that the images were image enhanced. Also, these images were recorded with the 35 mm digital camera. The double image of the unfiltered images is presented in Fig. 5a, which is highlighted by the droplet glare points. Figure 5b presents the droplet image when fluorescent dye is added to the droplet composition and one of the paired fluorescing images is resolved through the long-pass filter. The filtered image indicates that the Mie scattered light is blocked since the glare points are not present and the inelastic light that is transmitted through the filter is detected throughout the droplet volume.

With images as presented in Fig. 5, one can use this approach to detect a multitude of individual droplets generated by inhalers over a period of time. As mentioned earlier, optical patternators (using a laser sheet) image a spray cross section that includes an ensemble of fluorescing droplets. In this case, since the fluorescent dye is soluble in the liquid, the droplet ensemble contributes to measurement of the total fluorescence and scattering intensities at each camera pixel. The fluorescence signal of a droplet is then proportional to the concentration of the fluorescing molecules, as long as the dye is not at high enough concentration to cause self quenching. Therefore, the optical patternator can provide the two-dimensional spatial distribution of the liquid mass and Sauter mean diameter (i.e., ensemble volume-to-surface area diameter) [20, 21], which is the image ratio of the fluorescent intensity (proportional to the cube of the droplet diameter) and the scattered light signal (proportional to the diameter squared).

Unlike solutions with a soluble dye for which every formed droplet fluoresces, new drug multiphase formulations (e.g., suspension, emulsions) can become immiscible such that every droplet may not have the therapeutic agent, let alone the same agent concentration. Thus, the percentage of droplets with the therapeutic (i.e., the dosage) in an inhaler spray is unknown. One then needs to distinguish between droplets with and without the agent, i.e., detect the presence of droplets that do not fluoresce. The problem with ensemble average measurements, as with the optical patternator concept, is that it obscures the presence of non-fluorescing individual droplets. However, detecting individual droplets passing through a spatial region provides information on droplet fluorescent

distribution at that location with respect to droplet size, and can provide the delivered concentration with respect to the total liquid delivered.

Future Directions

Three issues that need to be addressed include 1) replacing the droplet array with an aerosol (and ultimately with commercial inhaler devices), 2) development of a cross-correlation algorithm to track paired droplet images (analogous to particle tracking in particle image velocimetery [23]), and 3) quantifying the fluorescence intensity of detected droplets. The cross-correlation algorithm is needed when the magnification is reduced so that the field-of-view includes many aerosol particles, and one needs to determine whether or not the particle image has a fluorescing mate. Quantification of the fluorescence signal would enable droplet-to-droplet variations in concentration of magnified droplets, and possibly determine the variation in agent concentration per droplet diameter.

Conclusions

A new methodology is described that can detect the concentration of active agent within individual droplets generated by pulmonary drug delivery devices. Images were presented to demonstrate how one might potentially carry out this task for commercially available inhalers by exploiting the use of fluorescing biomolecules.

Acknowledgements

Thanks to B. Johnson and N. Green for their assistance with the experimental arrangement and acquisition of results. Thanks to Dr. K.L. Steffens for helpful discussions concerning fluorescence measurements, and Dr. R.E. Cavicchi for help in synchronizing the laser and high-speed camera.

References

1. Shahani, S., *Advanced Drug Delivery Systems: Probing the Route to Growth New Developments, New Technologies, Companies and Trends*, Fuji-Keizai Publisher, 2005.
2. Puich, M., "Operations Excellence: The First Operational Roadmap for the Biopharmaceutical Industry," *BioPharm International*, pp. 16-17, 2006.
3. Filas, B., and Lengsfeld, C., "Mass Balance of Nebulized Drug Delivery: Residual Drug Levels and the Effects of an Alternative Air Humidification Method," *Atomization and Sprays*, Vol. 18, No. 6, pp. 495-510, 2008.
4. Loxley, A., and Dizdarevic, I., "Nebulizable Nanoparticle Dispersions: A Novel Inhalable Dosage Form," *Drug Delivery Technology*, Vol. 7, No. 8, pp. 42-45, 2007.
5. Amin, A., Shah, T., Patel, J., and Gajjar, A., "Non-Invasive Insulin: Annual Update on Non-Invasive Insulin Delivery Technologies," *Drug Delivery Technology*, Vol. 8, No. 3, pp. 43-48, 2008.
6. Sadrzadeh, N., Glembourtt, M.J., Stevenson, C.L., "Peptide Drug Delivery Strategies for the Treatment of Diabetes," *Journal of Pharmaceutical Sciences*, Vol. 96, Issue 8, pp. 1925-1954, 2007.
7. Dubin, C.H., "The State of systemic Pulmonary Delivery: One Year after Exubera's Approval," *Drug Delivery Technology*, Vol. 7, No. 4, pp. 61-67, 2007.
8. Patton, J.S., "The Potential and Promise for Pulmonary Delivery," Nektar Therapeutics, 2004.
9. van de Hulst, H.C., and Wang, R.T., " Glare Points," *Applied Optics*, Vol. 30, No. 33, pp. 4755-4763, 1991.

10. Yokoyama, H., Yamamura, Y., Ozeki, T., Iga, T., and Yamada, Y., "Analysis of Relationship between Peak Inspiratory Flow Rate and Amount of Drug Delivered to Lungs Following Inhalation of Fluticasone Propionate with a Diskhaler", *Biol. Pharm. Bull.*, Vol. 30, No. 1, pp. 162-164, 2007.
11. "Biopharmaceutical Drug Delivery," *BioPharm International Guide to Formulation, Fill, and Finish*, April 2004.
12. de Boer, A.H., Gjaltema, D., Hagedoorn, P., Schaller, M., Witt, W., Frijlink, H.W., "Design and Application of a New Modular Adapter for Laser Diffraction Characterization of Inhalation Aerosols," *International Journal of Pharmaceutics*, Vol. 249, No. 1, pp. 233-245, 2002.
13. DeHaana, W.H., Finlayb, W.H., "Predicting Extrathoracic Deposition from Dry Powder Inhalers, *Journal of Aerosol Science*, Vol. 35, pp. 309–331, 2004.
14. Adi, H., Traini, D., Chan, H.-K., Young, P.M., "The Influence of Drug Morphology on Aerosolisation Efficiency of Dry Powder Inhaler Formulations," *Journal of Pharmaceutical Sciences*, Published Online: 25 Sep 2007, DOI: 10.1002/jps.21195.
15. Craig, D.Q.M., and Reading M., "Spatially Resolved Characterisation of Dosage Forms using Novel Thermal Probe Techniques," *American Pharmaceutical Review*, Vol. 10, Issue 5, pp. 85-88, 2007.
16. "Guidance for Industry: Metered Dose Inhaler (MDI) and Dry Powder Inhaler (DPI) Drug Products - Chemistry, Manufacturing, and Controls Documentation," *US Department of Health and Human Services Food and Drug Administration*, Center for Drug Evaluation and Research (CDER), October 1998.
17. Lionberger, R.A., "Regulatory Aspects of the Use of New Particle Engineering Technologies," *American Pharmaceutical Review*, Vol. 10, Issue 5, pp. 80-84, 2007.
18. Sun, Y.-P., et al., "Quantum-Sized Carbon Dots for Bright and Colorful Photoluminescence," *Journal of the American Chemical Society*, Vol., 128, pp. 7756-7757, 2006.
19. Giepmans, B.N.G., Adams, S.R., Ellisman, M.H., and Tsien, R.Y., "The Fluorescent Toolbox for Assessing Protein Location and Function," *Science*, Vol. 312, pp. 217-224, 2006.
20. Talley, D.G., Thamban, A.T.S., McDonell, V.G., and Samuelsen, G.S., "Laser Sheet Visualization of Spray Structure," *Recent Advances in Spray Combustion: Spray Combustion Measurements and Model Simulation Volume II* (K.K. Kuo, editor), AIAA Progress in Astronautics and Aeronautics, Vol. 171, pp. 131-141, 1996.
21. Sankar, S.V. Mahler, K.E., Robart, D.M., and Bachalo, W.D., "Rapid Characterization of Fuel Atomizers Using an Optical Patternator", *Journal of Engineering for Gas Turbines and Power*, Vol. 121, pp. 409-414, 1999.
22. Patton, J.S., "Deep-Lung Delivery of Therapeutic Proteins," *ChemTech*, Vol. 27, No. 12, pp. 34-38, 1997.
23. Westerweel, J., "Fundamentals of Digital Particle Image Velocimetry," *Measurement Science and Technology*, Vol. 8, pp. 1379-1392, 1997.

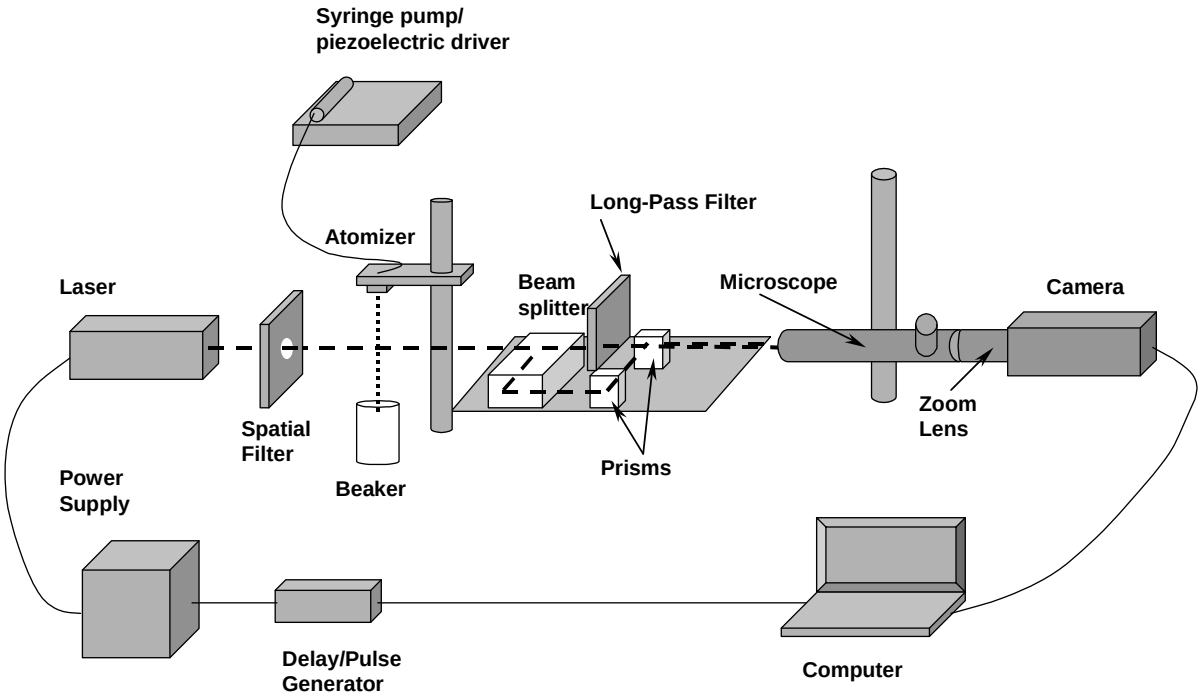

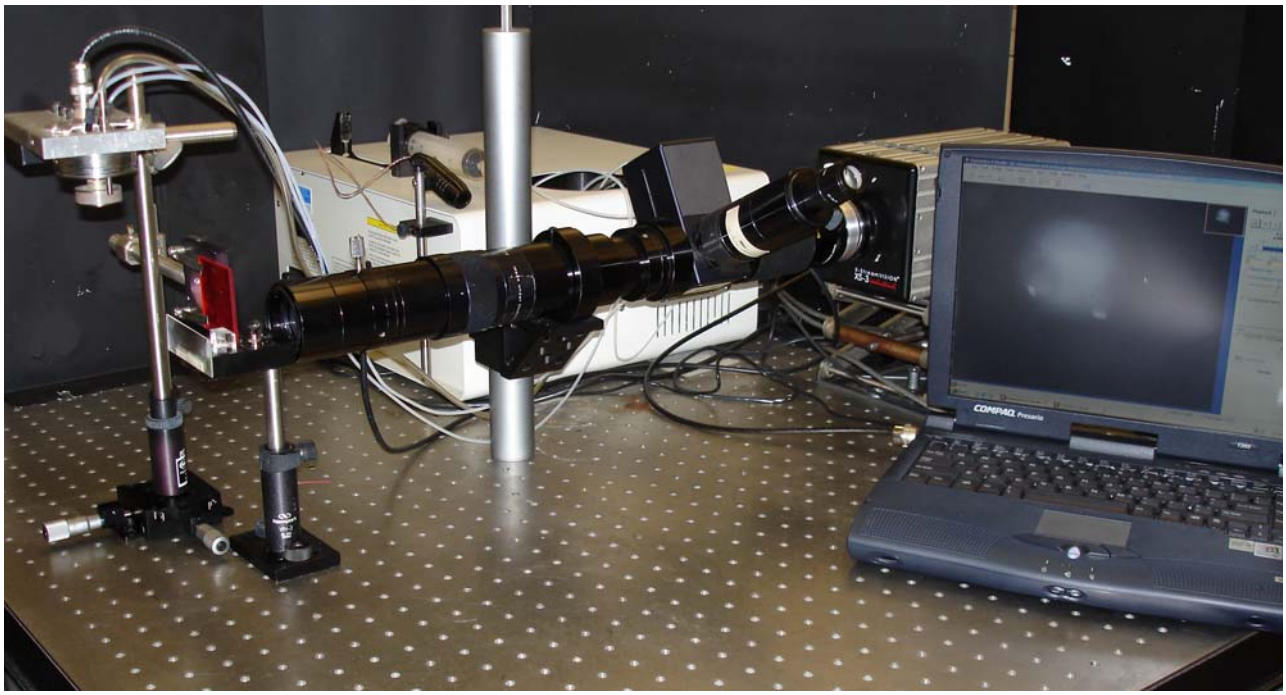

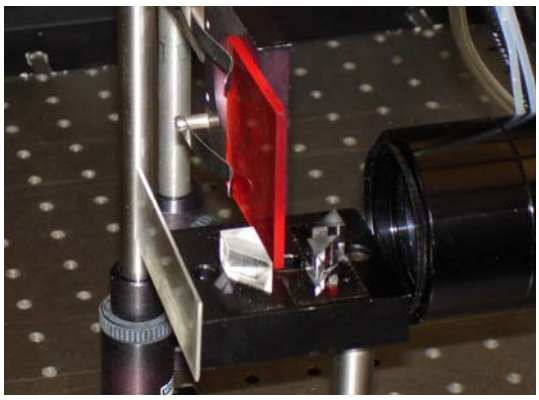

Fig. 1. Schematic and photograph of the experimental arrangement.

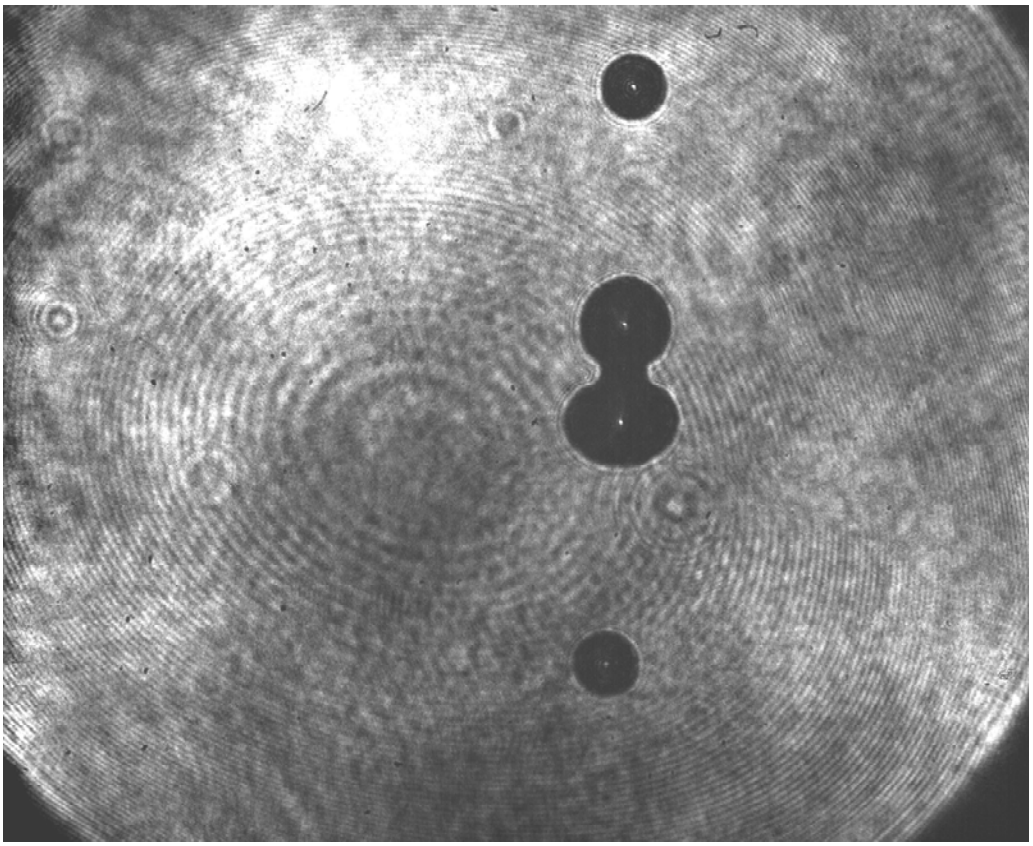

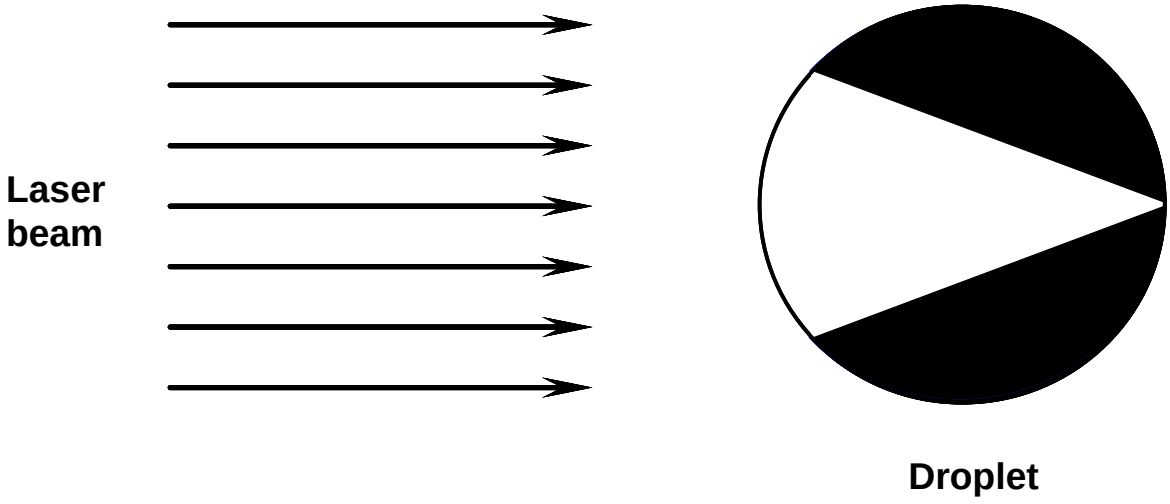

Fig. 2. Photograph of a single image of focused droplets using the array generator and laser backscatter illumination arrangement. The schematic illustrates how the laser light is focused through the droplet.

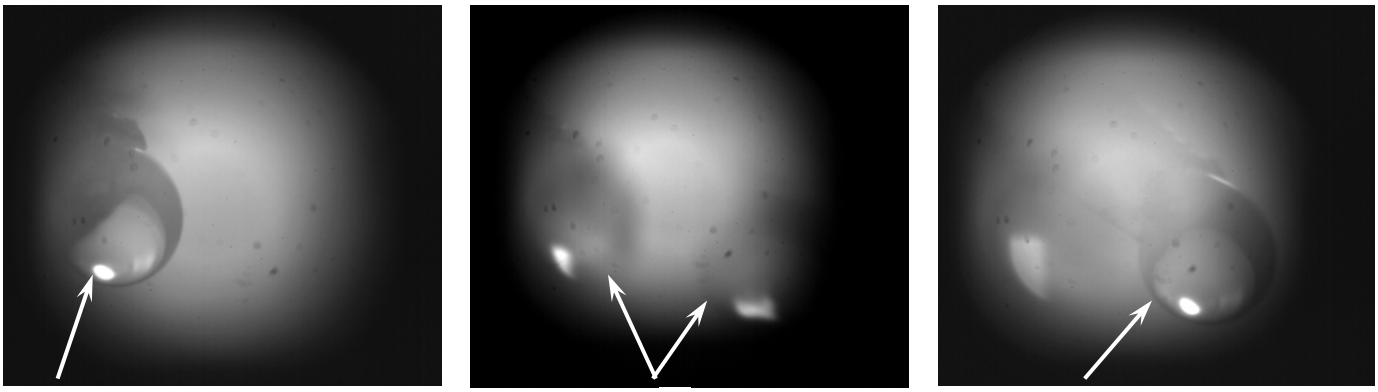

Fig. 3. Photograph of the double image of a pendent droplet with backscatter illumination from an incandescent lamp. Frames (a) and (c) present the focused single image, while Frame (b) shows the best focused view of both images.

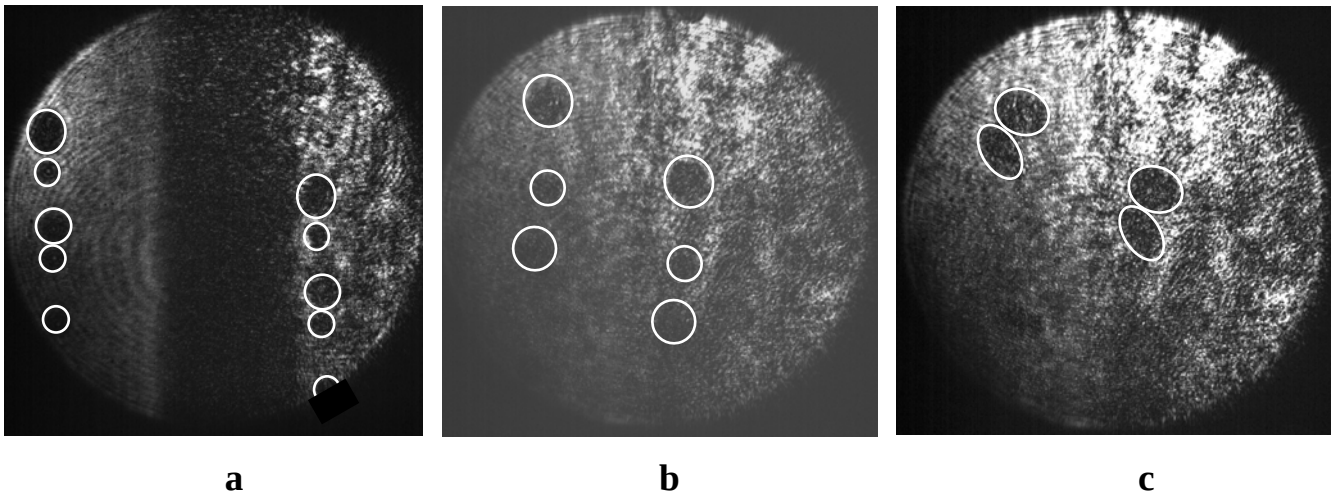

Fig. 4. Photographs of droplet double images using the array generator and laser backscatter illumination arrangement. The droplet images are highlighted by a white oval for clarity.

Fig. 5. Photographs of droplet double images using the array generator and laser 90° side-angle scattering arrangement: a) unfiltered Mie scattering and b) filtered arrangements.